Spinor Boltzmann equation approach to domain-wall motion driven by spin-polarized current

Ya-Ru Wang [1], Zheng-Chuan Wang [1,*] and Gang Su [1,2,†]

[1] *School of Physical Sciences, University of Chinese Academy of Sciences, Beijing 100049, People's Republic of China*

[2] *Kavli Institute for Theoretical Physics, CAS Center for Excellence in Topological Quantum Computation, University of Chinese Academy of Sciences, Beijing 100190, People's Republic of China*

(Received 31 October 2020; revised 8 February 2021; accepted 29 March 2021; published 9 April 2021)

Based on the nonequilibrium Green's function formalism, the spinor Boltzmann equation beyond gradient approximation is derived in a ferromagnetic metal with a single domain wall (DW). We further obtain the charge continuity equation and the spin diffusion equation by integrating over the momentum. By using the spin diffusion equation, we get a generalized spin transfer torque (STT), in which the usual STT is extended to the case beyond the gradient approximation and with inhomogeneous current. We also calculate numerically the physical observables such as charge density $n(x)$, spin accumulation $\boldsymbol{m}(x)$, current density $j(x)$, spin current density $\boldsymbol{j}_s(x)$, etc., by the use of the spinor distribution function. Along with the Landau-Lifshitz-Gilbert-Slonczewski equation that contains the above generalized STT, we can study the motion domain wall, and the critical electric field at an initial velocity of the DW is obtained in terms of the linear stability analysis method.

DOI: 10.1103/PhysRevB.103.144415

I. INTRODUCTION

In order to meet the increasing demand for ultradense storage devices, the operation of the domain wall (DW) by some external manipulations such as magnetic field, spin-polarized current, spin wave and temperature, etc., was proposed as a new type of magnetic memory [1–4]. The memory with current-induced DW moving via spin transfer torque (STT) has attracted more and more attention both in theoretical [5–7] and experimental [8,9] studies owing to its advantages in size, consumption, and speed. A magnetic domain is a region within a magnetic material in which the magnetization is in a uniform direction, and the boundary region of two domains is called the DW over which the magnetization changes its direction from one domain to another [10,11]. When a spin-polarized current passes through a DW, the STT, resulting from the *s-d* interaction of the conduction electron spins with the background magnetization of the DW, will cause the movement of the DW, which was called "domain drag force" by Berger [8,12,13].

In 2004, Li and Zhang [14] proposed a phenomenological form of STT produced by the spatial variation of spin current density in ferromagnetic materials to explore the movement of the DW, which reads $\boldsymbol{\tau}_b = -\frac{b_J}{M_s^2}\boldsymbol{M} \times (\boldsymbol{M} \times \frac{\partial \boldsymbol{M}}{\partial x})$, where $b_J = P j_e \mu_B/(eM_s)$, μ_B is the Bohr magneton, e is the electronic charge, j_e is the electronic current density, and P is the spin polarization of the current. Obviously, b_J is a coefficient related to P which should be determined by experiments. However, the current density j_e will change with the variation of the DW accordingly because the STT may affect the motion of both the DW and spin-polarized current, so we must deal with their movements simultaneously. To consider the varying spin-polarized current in the moving DW, Levy and colleagues [15,16] extended the above STT as $\boldsymbol{\tau}_{stt} = -\frac{\gamma}{\mu_B \mu_0} J_{ex} \int \boldsymbol{M} \times \boldsymbol{m}(x) dx$, where γ is the gyromagnetic ratio, μ_0 is the vacuum permeability, J_{ex} is the exchange coupling strength, and $\boldsymbol{m}(x)$ is the spin accumulation. The varying spin accumulation and spin current satisfy the spin diffusion equation that contains the STT therein. The spin diffusion equation can be derived from the spinor Boltzmann equation (SBE) naturally; in other words, we can also obtain the spin accumulation and spin current from SBE.

The quantum Boltzmann equation (QBE) is an important and powerful tool to investigate the transport process, and there has been much progress in recent years [17–20]. Based on Kadanoff's work on the QBE [21], Sheng *et al.* derived the SBE, including the spin degree of freedom in the steady state [22,23]. In order to study the behavior of the transverse spin current in noncollinear magnetic structures, Zhang *et al.* also proposed a time-dependent SBE in 2004 [24]. Wang further extended the form of SBE beyond the gradient approximation for describing the system with a rapid varying potential, which works whether the potentials vary slowly or rapidly with time and position [25], and then the charge current, spin current, and STT beyond the gradient approximation were investigated [26]. Nowadays, the SBE is widely used to study spin-dependent transport issues. Since the background magnetization in the DW will change rapidly when the DW moves, the usual SBE will fail to describe the spin-polarized electronic transport through the DW because the *s-d* interaction between conduction electrons and background magnetization varies rapidly, and we should study it using the SBE beyond the gradient approximation along with the Landau-Lifshitz-Gilbert-Slonczewski (LLGS) equation, where the LLGS equation describes the motion of magnetization.

This paper is organized as follows: In Sec. II we derive the SBE beyond the gradient approximation in a ferromagnetic

*wangzc@ucas.ac.cn
†gsu@ucas.ac.cn

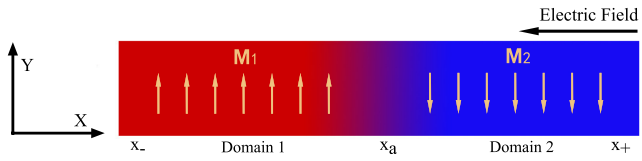

FIG. 1. The schematic structure of a ferromagnetic metal with a single DW. The directions of magnetization in the two domains are opposite; x_a represents the position of the DW, and the external electric field is along the $-x$ direction. Domain 1 is a pinnedlike layer which is used to polarize the spin of electrons. If the electric field exceeds the critical value, the DW will be driven by the STT induced by the spin-polarized current.

metal with a single DW and investigate the LLGS equation including STT using the method of linear stability analysis. In Sec. III we present the numerical results of charge density, spin accumulation, current density, and spin current density by calculating the SBE, and the critical electric field that drives the motion of the DW is obtained in terms of the linear stability analysis method for the LLGS equation. Finally, a summary and discussion is given.

II. THEORETICAL FORMALISM

Consider a ferromagnetic metal with a single DW, as shown in Fig. 1, where the spin-polarized electronic current flows through the x direction and drives the movement of the DW when an external electric field is applied along the x axis. Different DWs have different irregular shapes, which obey the principle of the lowest energy [12]. It is very hard to investigate both the motion of interacting spin-polarized electrons and the DW, which means we should solve the SBE and LLGS equation simultaneously. In order to simplify this problem, we ignore the thickness and type such as Bloch wall, Néel wall, etc., and describe the potential caused by the DW by a simple step function, then assume it moves at a certain speed.

The Hamiltonian for the electron in the ferromagnetic metal shown in Fig. 1 can be written as

$$\hat{H} = -\frac{\hbar^2\nabla_x^2}{2m_e} + eEx - \frac{1}{2}J_{ex}\boldsymbol{M}_1\cdot\hat{\boldsymbol{\sigma}}[\theta(x_a-x)-\theta(x_- - x)] - \frac{1}{2}J_{ex}\boldsymbol{M}_2\cdot\hat{\boldsymbol{\sigma}}[\theta(x-x_a)-\theta(x-x_+)], \quad (1)$$

where $-\frac{\hbar^2\nabla_x^2}{2m_e}$ is the kinetic energy of the electron, J_{ex} is the s-d exchange coupling constant, and $\boldsymbol{M}_1$ and $\boldsymbol{M}_2$ represent the unit vectors of the magnetization of ferromagnets in different domains, respectively. $\hat{\boldsymbol{\sigma}}$ are the Pauli spin matrices, the position x_a of the DW can be rewritten as $x_a = v_D t$ when we assume that the DW has a velocity v_D driven by the STT, and $(x_a - x_-)$ and $(x_+ - x_a)$ are the thicknesses of the left and right domains, respectively. $\theta(x)$ is the step function defined by

$$\theta(x) = \begin{cases} 1, & x < 0, \\ 0, & x > 0. \end{cases}$$

The spinor distribution function in spin space can be defined by a 2×2 matrix as

$$\hat{f}(\boldsymbol{k},\omega;\boldsymbol{x},t) = \begin{pmatrix} f_{\uparrow\uparrow}(\boldsymbol{k},\omega;\boldsymbol{x},t) & f_{\uparrow\downarrow}(\boldsymbol{k},\omega;\boldsymbol{x},t) \\ f_{\downarrow\uparrow}(\boldsymbol{k},\omega;\boldsymbol{x},t) & f_{\downarrow\downarrow}(\boldsymbol{k},\omega;\boldsymbol{x},t) \end{pmatrix},$$

where $\uparrow$ and $\downarrow$ are the spin indices, k is the wave vector, and ω is the frequency. As described in Ref. [24], the diagonal element $f_{\uparrow\uparrow}(\boldsymbol{k},\omega;\boldsymbol{x},t)$ [$f_{\downarrow\downarrow}(\boldsymbol{k},\omega;\boldsymbol{x},t)$] represents the occupancy of state $(\boldsymbol{k},\omega)$ and goes to the Fermi function in equilibrium so that only the spin state $\uparrow$ ($\downarrow$) is occupied, while the other is zero. In the two-fluid model, $f_{\uparrow\uparrow}$ and $f_{\downarrow\downarrow}$ can be considered to be independent of each other and related only to charge. The off-diagonal element $f_{\uparrow\downarrow}(\boldsymbol{k},\omega;\boldsymbol{x},t)$ [or $f_{\downarrow\uparrow}(\boldsymbol{k},\omega;\boldsymbol{x},t)$] represents the coherences between states $(\boldsymbol{k},\omega)$ on the Fermi surface and the states with opposite spin; these coherences can be induced by spin-polarized current. For this reason, the off-diagonal term is spin dependent [24]. The distribution function $f_{\sigma\sigma'}(\boldsymbol{k},\omega;\boldsymbol{x},t)$ is the quantum Wigner transformation of the lesser Green's function [26,27] in the nonequilibrium Green's function (NEGF) formalism:

$$\begin{aligned} &f_{\sigma\sigma'}(\boldsymbol{k},\omega;\boldsymbol{x},t) \\ &\quad = -iG^<_{\sigma\sigma'}(\boldsymbol{k},\omega;\boldsymbol{x},t) \\ &\quad = -i\int e^{-i\boldsymbol{k}\cdot\boldsymbol{\mathcal{X}}}\,d\boldsymbol{\mathcal{X}}\int e^{i\omega\mathcal{T}}G^<_{\sigma\sigma'}(\boldsymbol{\mathcal{X}},\mathcal{T};\boldsymbol{x},t)\,d\mathcal{T}, \end{aligned} \quad (2)$$

where $x = \frac{1}{2}(x_1+x_2)$, $t = \frac{1}{2}(t_1+t_2)$ is the center of mass variable, $\mathcal{X} = x_1 - x_2$, $\mathcal{T} = t_1 - t_2$ represent the differences between two position and time variables, and (x_1,t_1) and (x_2,t_2) are the position and time variables in the lesser Green's function $G^<_{\sigma\sigma'}(x_1,t_1;x_2,t_2)$.

Any 2×2 matrix can be decomposed into a new form by using the complete basis composed of the Pauli matrix $\hat{\boldsymbol{\sigma}}$ and unit matrix $\hat{\mathrm{I}}$. Based on the local equilibrium assumption, we further expand the spinor distribution function as [24,25]

$$\hat{f}(k,\omega;x,t) = f^0(k,\omega)\hat{\mathrm{I}} + \left(-\frac{\partial f^0}{\partial\epsilon}\right)[f(k,\omega;x,t)\hat{\mathrm{I}} + \boldsymbol{g}(k,\omega;x,t)\cdot\hat{\boldsymbol{\sigma}}], \quad (3)$$

where $f^0(k,\omega)$ is the equilibrium distribution function and $f(k,\omega;x,t)$ and $\boldsymbol{g}(k,\omega;x,t)$ are nonequilibrium scalar and vector distribution functions, respectively, which describe the deviation of the distribution function from the equilibrium distribution. Combining Eq. (3) with the original matrix of $\hat{f}(\boldsymbol{k},\omega;x,t)$ above, it can be found that the terms containing $\hat{\mathrm{I}}$ are exactly the diagonal elements $f_{\uparrow\uparrow}$ and $f_{\downarrow\downarrow}$, while the other terms containing $\hat{\boldsymbol{\sigma}}$ are exactly the off-diagonal elements $f_{\uparrow\downarrow}$ and $f_{\downarrow\uparrow}$. Therefore, the scalar distribution function f and the vector distribution function $\boldsymbol{g}$ are also interpreted as the charge distribution function and spin distribution function, respectively.

In the framework of Kadanoff *et al.*'s NEGF theory [21], starting from the Dyson equation satisfied by the Green's function and using a procedure similar to the derivation

of the QBE [28,29], as detailed in the Appendix, we can obtain coupled equations for the scalar distribution function $f(k,\omega;x,t)$ related to charge and the vector distribution function $\boldsymbol{g}(k,\omega;x,t)$ related to spin:

$$\begin{aligned}&\left(\frac{\partial}{\partial t}+\frac{\hbar k}{m_e}\frac{\partial}{\partial x}-\frac{eE}{\hbar}\frac{\partial}{\partial k}\right)f(k,\omega;x,t)+\frac{J_{ex}}{\hbar}\int\frac{1}{k'}\cos[2k'(v_Dt-x)](\boldsymbol{M}_1-\boldsymbol{M}_2)\cdot\boldsymbol{g}(k-k',\omega-k'v_D;x,t)\,dk'\\&\quad-\frac{J_{ex}}{\hbar}\int\frac{1}{k'}\{\boldsymbol{M}_1\cos[2k'(x_--x)]-\boldsymbol{M}_2\cos[2k'(x_+-x)]\}\cdot\boldsymbol{g}(k-k',\omega;x,t)\,dk'\\&\quad=-\frac{f(k,\omega;x,t)-\langle f\rangle}{\tau}\end{aligned}\tag{4}$$

and

$$\begin{aligned}&\left(\frac{\partial}{\partial t}+\frac{\hbar k}{m_e}\frac{\partial}{\partial x}-\frac{eE}{\hbar}\frac{\partial}{\partial k}\right)\boldsymbol{g}(k,\omega;x,t)+\frac{J_{ex}}{\hbar}\int\frac{1}{k'}\cos[2k'(v_Dt-x)](\boldsymbol{M}_1-\boldsymbol{M}_2)f(k-k',\omega-k'v_D;x,t)\,dk'\\&\quad+\frac{J_{ex}}{\hbar}\int\frac{1}{k'}\sin[2k'(v_Dt-x)](\boldsymbol{M}_1-\boldsymbol{M}_2)\times\boldsymbol{g}(k-k',\omega-k'v_D;x,t)\,dk'\\&\quad-\frac{J_{ex}}{\hbar}\int\frac{1}{k'}\{\boldsymbol{M}_1\cos[2k'(x_--x)]-\boldsymbol{M}_2\cos[2k'(x_+-x)]\}f(k-k',\omega;x,t)\,dk'\\&\quad-\frac{J_{ex}}{\hbar}\int\frac{1}{k'}\{\boldsymbol{M}_1\sin[2k'(x_--x)]-\boldsymbol{M}_2\sin[2k'(x_+-x)]\}\times\boldsymbol{g}(k-k',\omega;x,t)\,dk'\\&\quad=-\frac{\boldsymbol{g}(k,\omega;x,t)-\langle\boldsymbol{g}\rangle}{\tau}-\frac{2\langle\boldsymbol{g}\rangle}{\tau_{sf}},\end{aligned}\tag{5}$$

where k' represents the jump of momentum k when electrons are scattered. At first glance, mathematically, $k'=0$ is a singularity of the above coupled equations. But it is also a removable singularity. In order to prove the above argument, we calculated the limit of the integral terms in Eqs. (4) and (5) when k' tends to zero. We find it is zero, which will not have any effect on the result of the total integrals. Therefore, it is not necessary to consider $k'=0$ when doing numerical calculations, and we can remove this singularity. In fact, we can explain this from the physical point since k' denotes the momentum change in the conduction electron when it travels through the interface of two domains. The integral terms in Eqs. (4) and (5) contribute source terms scattered by the interface to the transport equations. While $k'=0$ means there is no scattering when the electron passes through the interface, its momentum does not change, so there are no contributions from the interface scattering to the source terms, which coincides with the above fact that the total integral terms is zero in the limit $k'\to 0$. So we do not consider the contribution $k'=0$ in our integral terms. Assuming that $j_1(k',x)=\frac{1}{k'}\cos[2k'(v_Dt-x)](\boldsymbol{M}_1-\boldsymbol{M}_2)$, j_1 can be interpreted as the transition probability of momentum and frequency from (k,ω) jumping to $(k-k',\omega-k'v_D)$ [27]. Similarly, if we assume that $j_2(k',x)=\frac{1}{k'}\{\boldsymbol{M}_1\cos[2k'(x_--x)]-\boldsymbol{M}_2\cos[2k'(x_+-x)]\}$, j_2 can be interpreted as the transition probability of the momentum and frequency from (k,ω) jumping to $(k-k',\omega)$. The physical explanation of other integral terms is similar to that of j_1 and j_2.

Integrating over the variables k and ω on both sides of Eq. (4), we can obtain the continuity equation of the charge density and current density as

$$\begin{aligned}&\frac{\partial}{\partial t}n(x,t)+\frac{\partial}{\partial x}j(x,t)+\frac{J_{ex}}{\hbar}\int\frac{1}{k'}\cos[2k'(v_Dt-x)](\boldsymbol{M}_1-\boldsymbol{M}_2)\cdot\boldsymbol{m}_{k'}(x,t)\,dk'\\&\quad-\frac{J_{ex}}{\hbar}\int\frac{1}{k'}\{\boldsymbol{M}_1\cos[2k'(x_--x)]-\boldsymbol{M}_2\cos[2k'(x_+-x)]\}\cdot\boldsymbol{m}_{k'}(x,t)\,dk'\\&\quad=-\frac{n(x,t)-\langle n\rangle}{\tau},\end{aligned}\tag{6}$$

where the charge density and the charge current density are defined as

$$n(x,t)=\iint\left(-\frac{\partial f^0}{\partial\epsilon}\right)f(k,\omega;x,t)\,dk\,d\omega\tag{7}$$

and

$$j(x,t)=\iint\left(-\frac{\partial f^0}{\partial\epsilon}\right)\frac{\hbar k}{m_e}f(k,\omega;x,t)\,dk\,d\omega.\tag{8}$$

Similarly, integrating over the variables k and ω on both sides of Eq. (5), we can obtain the spin diffusion equation of the spin accumulation and spin current density as

$$\begin{aligned}
&\frac{\partial}{\partial t}\boldsymbol{m}(x,t)+\frac{\partial}{\partial x}\boldsymbol{j}_s(x,t)+\frac{J_{ex}}{\hbar}\int\frac{1}{k'}\cos[2k'(v_Dt-x)](\boldsymbol{M}_1-\boldsymbol{M}_2)n_{k'}(x,t)\,dk'\\
&\quad+\frac{J_{ex}}{\hbar}\int\frac{1}{k'}\sin[2k'(v_Dt-x)](\boldsymbol{M}_1-\boldsymbol{M}_2)\times\boldsymbol{m}_{k'}(x,t)\,dk'\\
&\quad-\frac{J_{ex}}{\hbar}\int\frac{1}{k'}\{\boldsymbol{M}_1\cos[2k'(x_--x)]-\boldsymbol{M}_2\cos[2k'(x_+-x)]\}n_{k'}(x,t)\,dk'\\
&\quad-\frac{J_{ex}}{\hbar}\int\frac{1}{k'}\{\boldsymbol{M}_1\sin[2k'(x_--x)]-\boldsymbol{M}_2\sin[2k'(x_+-x)]\}\times\boldsymbol{m}_{k'}(x,t)\,dk'\\
&=-\frac{\boldsymbol{m}(x,t)-\langle\boldsymbol{m}\rangle}{\tau}-\frac{2\langle\boldsymbol{m}\rangle}{\tau_{sf}},
\end{aligned}\tag{9}$$

where the spin accumulation and spin current density are defined as

$$\boldsymbol{m}(x,t)=\iint\left(-\frac{\partial f^0}{\partial\epsilon}\right)\boldsymbol{g}(k,\omega;x,t)\,dk\,d\omega\tag{10}$$

and

$$\boldsymbol{j}_s(x,t)=\iint\left(-\frac{\partial f^0}{\partial\epsilon}\right)\frac{\hbar k}{m_e}\boldsymbol{g}(k,\omega;x,t)\,dk\,d\omega\tag{11}$$

and j_{s_i} is the i_{th} spin component of the current density along the x direction.

We denote $n_{k'}(x)=\int f(k-k',\omega;x,t)\,dkd\omega$ and $\boldsymbol{m}_{k'}(x)=\int\boldsymbol{g}(k-k',\omega;x,t)\,dkd\omega$ in Eqs. (6) and (9) as the charge density because it is related to the scalar distribution and spin accumulation, which is related to the vector distribution function corresponding to the momentum jump k'. So Eq. (6) is just the continuity equation for charge density and charge current density, and Eq. (9) is the continuity equation for spin accumulation and spin current density.

As we know, when the time is longer than the spin-flip relaxation of electrons τ_{sf}, it is reasonable to considered that the system will arrive at a steady state; then the spin accumulation, spin current density, and charge density will satisfy the following equations: $\frac{\partial}{\partial t}\boldsymbol{m}(x,t)=0$, $\frac{\partial}{\partial t}\boldsymbol{j}_s(x,t)=0$, and $\frac{\partial}{\partial t}n(x,t)=0$, respectively. For simplicity the time dependence of the spin accumulation, spin current density, and charge density can be approximated as $\boldsymbol{m}(x,t)=\boldsymbol{m}(x)(1+e^{-\frac{t}{\tau_{sf}}})$, $\boldsymbol{j}_s(x,t)=\boldsymbol{j}_s(x)(1+e^{-\frac{t}{\tau_{sf}}})$, and $n(x,t)=n(x)(1+e^{-\frac{t}{\tau}})$; it is easy to prove that the above physical quantities will eventually transition to $\boldsymbol{m}(x,t)\propto\boldsymbol{m}(x)$, $\boldsymbol{j}_s(x,t)\propto\boldsymbol{j}_s(x)$, and $n(x,t)\propto n(x)$ when $t\gg\tau_{sf}$, where $\boldsymbol{m}(x)$, $\boldsymbol{j}_s(x)$, and $n(x)$ are the spin accumulation, spin current density, and charge density when the system arrives at the steady state, respectively. Inserting $\boldsymbol{m}(x,t)$, $\boldsymbol{j}_s(x,t)$, and $n(x,t)$ at steady state into the spin diffusion equation (9), the spin accumulation can be expressed in the steady state as

$$\begin{aligned}
\boldsymbol{m}(x)=&-\tau\frac{\partial}{\partial x}\boldsymbol{j}_s(x)-(1-\lambda)\langle\boldsymbol{m}\rangle-\xi\int\frac{1}{k'}\cos[2k'(v_Dt-x)](\boldsymbol{M}_1-\boldsymbol{M}_2)n_{k'}(x)\,dk'\\
&-\xi\int\frac{1}{k'}\sin[2k'(v_Dt-x)](\boldsymbol{M}_1-\boldsymbol{M}_2)\times\boldsymbol{m}_{k'}(x)\,dk'+\xi\int\frac{1}{k'}\{\boldsymbol{M}_1\cos[2k'(x_--x)]-\boldsymbol{M}_2\cos[2k'(x_+-x)]\}n_{k'}(x)\,dk'\\
&+\xi\int\frac{1}{k'}\{\boldsymbol{M}_1\sin[2k'(x_--x)]-\boldsymbol{M}_2\sin[2k'(x_+-x)]\}\times\boldsymbol{m}_{k'}(x)\,dk',
\end{aligned}\tag{12}$$

where $\xi=\tau\frac{J_{ex}}{\hbar}$ is dimensionless. The spin accumulation in equilibrium $\langle\boldsymbol{m}\rangle$ is parallel to the magnetization.

Substituting Eq. (12) into the definition of STT $\boldsymbol{\tau}_{stt}=-\frac{\gamma}{\mu_B\mu_0}J_{ex}\int\boldsymbol{M}\times\boldsymbol{m}(x)\,dx$ proposed by Levy and colleagues [15,16], we have

$$\begin{aligned}
\boldsymbol{\tau}_{stt}=&c_J\tau\int\boldsymbol{M}\times\frac{\partial}{\partial x}\boldsymbol{j}_s(x)\,dx+c_J\xi\int dx\int\frac{1}{k'}\cos[2k'(v_Dt-x)]\boldsymbol{M}\times(\boldsymbol{M}_1-\boldsymbol{M}_2)n_{k'}(x)\,dk'\\
&+c_J\xi\int dx\int\frac{1}{k'}\sin[2k'(v_Dt-x)]\boldsymbol{M}\times[(\boldsymbol{M}_1-\boldsymbol{M}_2)\times\boldsymbol{m}_{k'}(x)]\,dk'\\
&-c_J\xi\int dx\int\frac{1}{k'}\boldsymbol{M}\times\{\boldsymbol{M}_1\cos[2k'(x_--x)]-\boldsymbol{M}_2\cos[2k'(x_+-x)]\}n_{k'}(x)\,dk'\\
&-c_J\xi\int dx\int\frac{1}{k'}\boldsymbol{M}\times(\{\boldsymbol{M}_1\sin[2k'(x_--x)]-\boldsymbol{M}_2\sin[2k'(x_+-x)]\}\times\boldsymbol{m}_{k'}(x))\,dk',
\end{aligned}\tag{13}$$

where $c_J = \frac{\gamma}{\mu_B \mu_0} J_{ex}$ has units of frequency. It can be seen above that the STT includes the following terms: the first term is caused by the variation of the spin current in space, which is analogous to the phenomenological form of the STT $\boldsymbol{\tau}_b \equiv \frac{\partial}{\partial x}\boldsymbol{j}_s(x)$ proposed by Li an Zhang [14], but our expression is derived analytically; the third and fifth terms are similar to the generalized torque $\boldsymbol{\tau}^{\pm}$ defined by Wang [26]. The second and fourth terms are the added terms in this work, which indicate that the charge density also makes a contribution to the STT. Equation (13) contains not only the position-dependent STT given by Li and Zhang [14] but also the momentum-dependent STT extended by Wang [26], and two additional terms associated with charge density also appear. Equation (13) is the central result here.

This STT not only affects the motion of conduction electrons but also influences the movement of the DW, which can be described by the LLGS equation, which means the STT will appear in the LLGS equation,

$$\frac{\partial \boldsymbol{M}}{\partial t} = -\gamma \boldsymbol{M} \times \boldsymbol{H}_{\text{eff}} + \frac{\alpha}{M_s}\boldsymbol{M} \times \frac{\partial \boldsymbol{M}}{\partial t} + \boldsymbol{\tau}_{stt}, \tag{14}$$

where α is the Gilbert damping coefficient and M_s is the saturation magnetization. The first term on the right-hand side of Eq. (14) describes the torque on the local magnetic moment due to all the effective fields in the system including the effective anisotropy field $\boldsymbol{H}_k$ and the exchange field $\boldsymbol{H}_{ex}$ between adjacent magnetizations. The second term describes the effect of the magnetic damping on the precession of the moment [11]. The third term is the STT given by Eq. (13). In our model we write $\boldsymbol{H}_{\text{eff}}$ as

$$\boldsymbol{H}_{\text{eff}} = \boldsymbol{H}_k + \boldsymbol{H}_{ex} = \frac{H_k M_y}{M_s}\boldsymbol{e}_y + \frac{2A_{ex}}{\mu_0 M_s^2}\nabla^2 \boldsymbol{M}, \tag{15}$$

where H_k is the anisotropy field and A_{ex} is the exchange constant.

The SBEs (4) and (5) and the LLGS equation (14) should be solved simultaneously; that is difficult because the equations are very complex, so we must adopt some approximations to solve these coupled equations. As we know, the relaxation time of conduction electrons (including momentum relaxation τ and spin-flip relaxation τ_{sf}) is much smaller than that of the magnetization of the background ferromagnet, where the former is of the order of picoseconds ($\tau \approx 0.001$ ps, $\tau_{sf} \approx 1$ ps) and the latter is about 1 ns [30]. This result strongly shows that the motion of the local magnetic moment is much slower than that of conduction electrons. It is useful to make some simplifications to solve the coupled equations (4), (5), and (14) based on the above fact. The principle one is recognizing that the conduction electronic spin redistribution occurs much faster than the motion of the background ferromagnet, so that one can envisage a time period in which the electronic spin accumulation has reached a quasisteady state before the magnetization of the local ferromagnetic starts to develop; that is, we can start the time development of the magnetization of the background ferromagnet after the electronic spin accumulation has reached steady state, which is called the adiabatic approximation [31]. Since the charge density and spin density of conduction electrons satisfy their continuity equations derived from the SBE, which can be solved at the steady state corresponding to a magnetization which obeys the LLGS equation at some time, at each time of magnetization, we solve the SBE for electrons at the corresponding steady state and then repeat this procedure for the next time. Thus, we can study both the motion of electrons and the magnetization of local ferromagnet simultaneously. Therefore, we first solve the SBEs (4) and (5) at steady state numerically, and after obtaining the spinor distribution function and the STT, we substitute them into the LLGS equation (14). The solution for the motion of the domain wall satisfies the LLGS equation. In this paper, we will not solve the LLGS equation but will study the critical electric field E_c driving the motion of the DW using the linear stability analysis method, then determine the initial velocity of the DW v_D, where the whole procedure must be performed self-consistently.

The linear stability analysis was used to study the DW dynamics with STT by Li and Zhang in 2004 [14]. Here, we exploit the STT given by Eq. (13) instead of the previous phenomenological form in Ref. [14]. Although we have not solved the LLGS equation directly, we can obtain the critical electronic current or the critical electric field which drives the DW to start to move from an initial state $\boldsymbol{M}_{20} = M_s(0, -1, 0)$. When we apply an electric field to the system, the STT induced by the spin-polarized current will produce a perturbation $\delta \boldsymbol{M}$ on the DW. If the electric field is lower than the critical electric field E_c, the DW still remains unchanged; if the electric field exceeds the critical electric field E_c, the DW will lose its stability and begin to move with an initial velocity v_D. Consider one component of perturbation with wave vector K and frequency Ω, where $v_D = \frac{\Omega}{K}$, by means of the method of linear stability analysis given by Lyapounov [32,33]; the solution of the LLGS equation on the right ferromagnet of the DW can be written as

$$\boldsymbol{M}(x, t) = \boldsymbol{M}_{20} + \delta \boldsymbol{M} = -M_s \boldsymbol{e}_y + \boldsymbol{u} e^{i(Kx + \Omega t)}, \tag{16}$$

where $\boldsymbol{M}_{20} = M_s(0, -1, 0)$ and $\boldsymbol{u}$ is a small vector representing the amplitude of the perturbation.

Substituting Eqs. (15) and (16) into Eq. (14) and keeping the linear terms in $\boldsymbol{u}$, the equations for the amplitude $\boldsymbol{u}$ can be obtained:

$$\begin{aligned} i\Omega u_x &= I_z u_y + (\gamma_k - \gamma_{ex} K^2 - I_y - i\alpha\Omega) u_z, \\ i\Omega u_y &= I_x u_z - I_z u_x, \\ i\Omega u_z &= -(\gamma_k - \gamma_{ex} K^2 - I_y - i\alpha\Omega) u_x - I_x u_y, \end{aligned} \tag{17}$$

where $\gamma_{ex} = \gamma \frac{2A_{ex}}{\mu_0 M_s}$ and $\gamma_k = \gamma H_k$ are the physical constants related to the material parameters, $I_{x,y,z} = -c_J \int m_{x,y,z}(x)\, dx$, and $m_{x,y,z}(x)$ are the components of spin accumulation. To obtain the nonzero solutions of $\boldsymbol{u}$, one should require the determinant of the coefficients for the linear equations to be zero, which is just the characteristic equation for Ω at a certain $K = \frac{\Omega}{v_D}$ and reads

$$\Omega^2 - (\gamma_k - \gamma_{ex} K^2 - I_y - i\alpha\Omega)^2 - \left(I_x^2 + I_z^2\right) = 0. \tag{18}$$

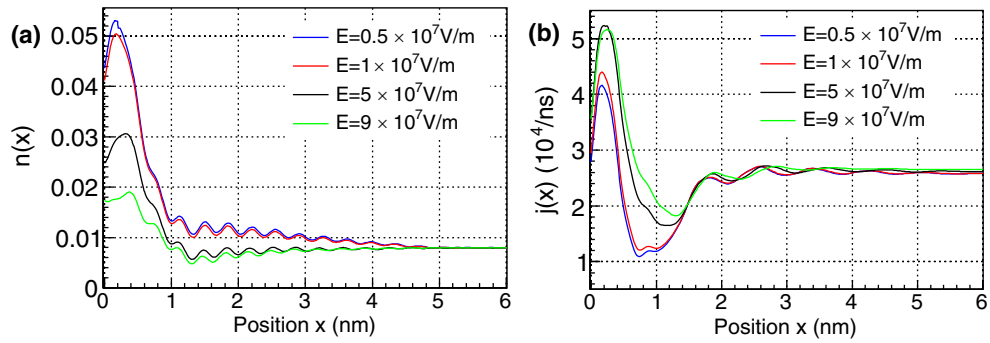

FIG. 2. The charge density and charge current density on the right side of the DW (domain 2) vary with position under different electric fields. (a) The charge density versus position. (b) The charge current density versus position.

By further substituting $K = \frac{\Omega}{v_D}$ into the above equation we can get a quartic function for Ω. Equation (18) becomes

$$\gamma_{ex}^2 \frac{\Omega^4}{v_D^4} + 2i\alpha\gamma_{ex}\frac{\Omega^3}{v_D^2} - 2\gamma_{ex}(\gamma_k - I_y)\frac{\Omega^2}{v_D^2} - (1+\alpha^2)\Omega^2 + 2i\alpha(\gamma_k - I_y)\Omega + (\gamma_k - I_y)^2 + I_x^2 + I_z^2 = 0. \quad (19)$$

There are four characteristic values for Ω. If we divide the complex roots into the real part a_j and imaginary part b_j, we have $\Omega_j = a_j + ib_j$ $(j = 1, 2, 3, 4)$. According to the principle of linearized stability proposed by Lyapounov [32,33], if all the characteristic values Ω_j have positive imaginary parts, then $\boldsymbol{M}_{20} = M_s(0, -1, 0)$ is a stable equilibrium solution. If some characteristic values Ω_j have negative imaginary parts, then $\boldsymbol{M}_{20} = M_s(0, -1, 0)$ loses its stability and begins to move with an initial velocity v_D. The critical point corresponds to the zero imaginary part of characteristic values. Therefore, we can obtain the critical electric field E_c and the initial velocity of the DW v_D by observing whether the imaginary part of the root b_j is zero. We will demonstrate this with an example in the next section.

III. NUMERICAL RESULTS

In our calculations, the magnetizations of the background ferromagnet in the two domains are taken as $\boldsymbol{M}_1 = M_s(0, 1, 0)$ and $\boldsymbol{M}_2 = M_s(0, -1, 0)$. We take the adiabatic approximation and assume that the distribution function of the electrons will arrive at a steady state $\frac{\partial \hat{f}}{\partial t} = 0$ after $t \gg \tau_{sf}$. For simplicity, we will not consider the frequency ω dependence in the distribution function. We choose the Fermi-Dirac distribution to be the equilibrium distribution of the scalar distribution function $\langle f(k, x)\rangle = f_{FD}(k)$ and the boundary conditions to be $\hat{f}(k, x_-) = \hat{f}(k, x_+) = 0$. We consider only the electrons near the Fermi surface, which contribute mainly to the transport. Other parameters in the system are chosen to be $J_{ex} = 0.5$ eV, $x_- = -10$ nm, $x_+ = 10$ nm, $\tau = 0.001$ ps, $\tau_{sf} = 1$ ps.

We solve Eqs. (4) and (5) numerically and show some physical observables such as charge density $n(x)$, charge current density $j(x)$, spin accumulation $\boldsymbol{m}(x)$, and spin current density $\boldsymbol{j}_s(x)$ in Figs. 2 and 3.

In Fig. 2, we plot the distribution of the charge density $n(x)$ and charge current density $j(x)$ in domain 2 as a function of position. The blue, red, black, and green curves correspond to the parameters $(E, v_D) = (0.5 \times 10^7$ V/m, 0 m/s), $(E, v_D) = (1 \times 10^7$ V/m, 0 m/s), $(E, v_D) = (5 \times 10^7$ V/m, 9.9×10^{-8} m/s), and $(E, v_D) = (9 \times 10^7$ V/m, 9.9×10^{-8} m/s), respectively. Since the critical electric field obtained (shown in Fig. 4 below) is $E_c = 4.92 \times 10^7$ V/m, the velocity of the DW is zero when $E < E_c$. The charge density under different electric fields in Fig. 2(a) has similar features, which first increases rapidly and then exhibits an oscillating decay with position. Because we presume the step function potential in our model is between domain 1 and domain 2, the charge accumulation is produced near the DW. It can be seen that the variation of the blue and red curves with position is more drastic than the other two curves; in the latter the electric fields are larger than the critical electric field. For the case of the blue and red curves with $E < E_c$, the DW does not move, and the charge current density is smaller than in the cases with $E > E_c$ when the DW starts to move (see Fig. 2), so there is a big charge accumulation in this case. In Figs. 2(a) and 2(b), the blue line and the red line almost overlap, and the black line and the green line also show little difference. It can be seen that when $E < E_c$ ($\approx 5 \times 10^7$ V/m), there is almost no difference in charge density $n(x)$ [charge current density $j(x)$] under different electric fields, and the same is true for $Ec \leqslant E \leqslant 9 \times 10^7$ V/m. This result means that $n(x)$ [$j(x)$] changes significantly only when E reaches E_c. Moreover, it is known from our calculation that the numerical results of these physical quantities will diverge when $E > 9 \times 10^7$ V/m, which indicates that the critical electric field must be less than 9×10^7 V/m.

The x, y, and z components of the spin accumulation under different electric fields are shown in Figs. 3(a)–3(c), which are similar to the charge accumulation. To manifest them clearly, we show the local enlarged curves of the spin accumulation near the DW in the inset of Figs. 3(a)–3(c), and it is easy to see that the x and z components of the spin accumulation under different electric fields oscillates only near the DW and then remains unchanged in the region $x > 0.4$ nm, while the y component of the spin accumulation increases to the maximum, then rapidly declines to the minimum, and gradually tends to zero. Because the directions of the magnetization on both sides of the DW shown in Fig. 1 are opposite along the y axis, a big spin accumulation exists near the DW which exerts STT on the right-hand side of the DW. The x and z components

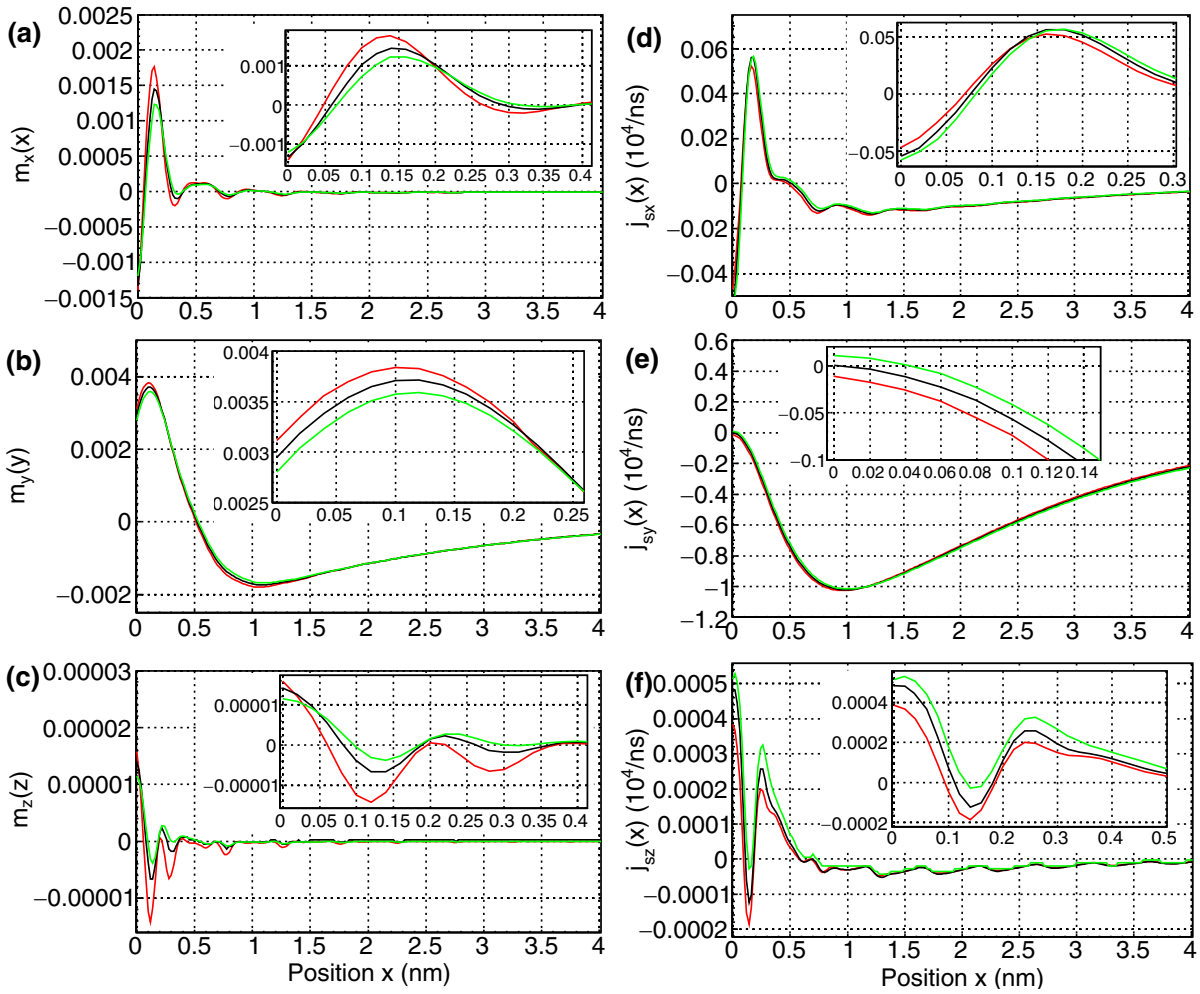

FIG. 3. The x, y, and z components of spin accumulation and spin current density as a function of position at different electric fields; the red, black, and green curves correspond to the parameters $(E, v_D) = (1 \times 10^7$ V/m, 0 m/s), $(E, v_D) = (5 \times 10^7$ V/m, 9.9×10^{-8} m/s), and $(E, v_D) = (9 \times 10^7$ V/m, 9.9×10^{-8} m/s), respectively. (a)–(c) The spin accumulation versus position. (d)–(f) The spin current density versus position.

of the spin accumulation have smaller magnitudes than that along the y component, as the magnetization of the ferromagnet is assumed along the y axis, and the x and z components of the spin accumulation have almost no effect on the entire transport.

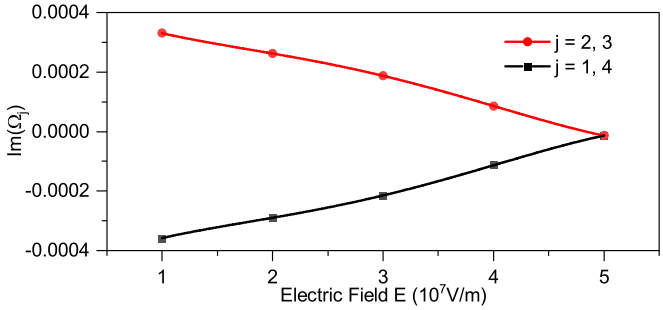

FIG. 4. The imaginary part b_j of the roots Ω_j in Eq. (19) versus electric field. It turns out that the critical condition $b_j = 0$ is satisfied when the electric field arrives at 4.92×10^7 V/m.

For comparison, we also plot the x, y, and z components of spin current density $\boldsymbol{j}_s(x)$ with position under different electric fields in Figs. 3(d)–3(f). When the electric field $E < E_c$, the spin current is smaller than in the case of $E > E_c$, while the spin accumulation is bigger than in the case of $E > E_c$, which is analogous to the charge accumulation. The magnitudes of the x and z components of the spin current density are smaller than that of the y component of the spin current density, in which the z component is the smallest, which is consistent with the results of spin accumulation.

We substitute the vector distribution function $g_{x,y,z}(k, x)$ under different (E, v_D) in Eq. (19) and adopt the parameters in this system as $H_k = 10$ Oe, $\gamma = 1.75 \times 10^7$ Oe^{-1} s^{-1}, $M_s = 8 \times 10^5$ A/m, $A = 1.3 \times 10^{-11}$ J/m, $\alpha = 0.02$, and $\mu_B = 9.274 \times 10^{-24}$ A m^2. Then the roots of Eq. (19) at a certain parameter (E, v_D) can be obtained self-consistently. In Fig. 4 we show how $b_j (j = 1, 2, 3, 4)$ varies with the electric field E.

We found that when the velocity of the DW v_D is greater than 9.9×10^{-8} m/s, the imaginary parts of Ω_j are all

negative regardless of the different electric fields. This indicates that the DW has lost its stability according to the principle of linear stability presented in Sec. II. As can be seen from Fig. 4, the imaginary parts of Ω will tend to zero at the point $E = 4.92 \times 10^7$ V/m, which means that it is just the critical field when v_D is taken to be 9.9×10^{-8} m/s.

IV. SUMMARY AND DISCUSSION

In this paper, we derived the SBE given in Eqs. (4) and (5) beyond the gradient approximation in a ferromagnetic metal with the single DW, and the continuity equation of charge density (6) and the spin diffusion equation (9) satisfied by the spin accumulation were also given. From the spin diffusion equation we further obtained a generalized STT under a steady-state assumption which contains terms associated with the charge density. Then we calculated the scalar distribution function $f(k, x)$ and the vector distribution function $\boldsymbol{g}(k, x)$ as well as some physical observables numerically. The results for the charge density $n(x)$, current density $j(x)$, spin accumulation $\boldsymbol{m}(x)$, and spin current density $\boldsymbol{j}_s(x)$ under different electric fields and velocity (E, v_D) are shown in Figs. 2 and 3. Moreover, we substituted the generalized STT into the LLGS equation (14) and obtained the critical electric field by means of linear stability analysis. By performing the self-consistent calculations with the SBE, we finally obtained the critical electric field $E_c = 4.92 \times 10^7$ V/m at the initial velocity of DW $v_D = 9.9 \times 10^{-8}$ m/s.

It should be emphasized that we should solve both the coupled SBE for conducting electrons and the LLGS equation for the DW simultaneously, but that is hard. For simplicity, we studied the LLGS equation using the method of linear stability analysis. Although we could obtain the critical electric field at an initial velocity, we failed to get the complete solution for the motion of the DW. How to solve the coupled SBE and LLGS equation self-consistently is an open question, which we will leave for further exploration.

ACKNOWLEDGMENTS

This study is supported by the National Key R&D Program of China (Grant No. 2018YFA0305800), NSFC (Grant No. 11834014), and the Strategic Priority Research Program of the Chinese Academy of Sciences (Grant No. XDB28000000). We also thank Prof. Z.-G. Zhu and B. Gu for their helpful discussions.

APPENDIX: DERIVATION OF THE SBE BEYOND THE GRADIENT APPROXIMATION

In this Appendix we will present the detailed derivation of Eqs. (4) and (5).

We start with Dyson's equation satisfied by $\hat{G}^<(x_1, x_2)$, that is, the starting point for the derivation of the QBE [21,28]. The variables are changed to center of mass $x_{1,2} = x \pm \mathcal{X}, t_{1,2} = t \pm \mathcal{T}$, and then the relative coordinates $(\mathcal{X}, \mathcal{T})$ are Fourier transformed to (k, ω). Finally, the equation of motion for $\hat{G}^<(k, \omega; x, t)$ is presented naturally:

$$
\begin{aligned}
&i\hbar\left[\frac{\partial}{\partial t} + \frac{\hbar k}{m_e}\nabla_x - \frac{eE}{\hbar}\nabla_k\right]\hat{G}^<(k,\omega;x,t) \\
&\quad + \frac{J_{ex}}{2}\int d\mathcal{X}\, e^{-ik\mathcal{X}}\int d\mathcal{T}\, e^{i\omega\mathcal{T}}\boldsymbol{M}_1\cdot\hat{\boldsymbol{\sigma}}\hat{G}^<(\mathcal{X},\mathcal{T};x,t)\left\{\theta\left[v_D\left(t+\frac{\mathcal{T}}{2}\right)-x-\frac{\mathcal{X}}{2}\right]-\theta\left(x_- - x-\frac{\mathcal{X}}{2}\right)\right\} \\
&\quad - \frac{J_{ex}}{2}\int d\mathcal{X}\, e^{-ik\mathcal{X}}\int d\mathcal{T}\, e^{i\omega\mathcal{T}}\hat{G}^<(\mathcal{X},\mathcal{T};x,t)\boldsymbol{M}_1\cdot\hat{\boldsymbol{\sigma}}\left\{\theta\left[v_D\left(t-\frac{\mathcal{T}}{2}\right)-x+\frac{\mathcal{X}}{2}\right]-\theta\left(x_- - x+\frac{\mathcal{X}}{2}\right)\right\} \\
&\quad + \frac{J_{ex}}{2}\int d\mathcal{X}\, e^{-ik\mathcal{X}}\int d\mathcal{T}\, e^{i\omega\mathcal{T}}\boldsymbol{M}_2\cdot\hat{\boldsymbol{\sigma}}\hat{G}^<(\mathcal{X},\mathcal{T};x,t)\left\{\theta\left[x+\frac{\mathcal{X}}{2}-v_D\left(t+\frac{\mathcal{T}}{2}\right)\right]-\theta\left(x+\frac{\mathcal{X}}{2}-x_+\right)\right\} \\
&\quad - \frac{J_{ex}}{2}\int d\mathcal{X}\, e^{-ik\mathcal{X}}\int d\mathcal{T}\, e^{i\omega\mathcal{T}}\hat{G}^<(\mathcal{X},\mathcal{T};x,t)\boldsymbol{M}_2\cdot\hat{\boldsymbol{\sigma}}\left\{\theta\left[x-\frac{\mathcal{X}}{2}-v_D\left(t-\frac{\mathcal{T}}{2}\right)\right]-\theta\left(x-\frac{\mathcal{X}}{2}-x_+\right)\right\} \\
&= \int d\mathcal{X}\, e^{-ik\mathcal{X}}\int d\mathcal{T}\, e^{i\omega\mathcal{T}}\int dx_3\,[\Sigma_t G^< - \Sigma^< G_{\bar{t}} - G_t\Sigma^< + G^<\Sigma_{\bar{t}}],
\end{aligned}
\tag{A1}
$$

where the Green's functions $G^<$, G_t, and $G_{\bar{t}}$ and the self-energies $\Sigma^<$, Σ_t, and $\Sigma_{\bar{t}}$ are 2×2 matrices in spin space. Obviously, the terms of the Fourier transformation on the left side of Eq. (A1) contain a discontinuous potential, so we cannot use the usual gradient approximation which applies to potentials varying slowly with time and position. We treat the integral terms of Eq. (A1) that contain a discontinuous potential in a formula proposed by Wigner in 1932 to deal with convolution with rapidly varying potentials [27], and Wang derived the SBE beyond the gradient approximation in a ferromagnet/insulator/ferromagnet (F/I/F) junction by using this formula [25]. We choose one of the integral terms to show this treatment in the following:

$$
I = \frac{J_{ex}}{2}\int d\mathcal{X} e^{-ik\mathcal{X}}\int d\mathcal{T} e^{i\omega\mathcal{T}}\boldsymbol{M}_1\cdot\hat{\boldsymbol{\sigma}}\hat{G}^<(\mathcal{X},\mathcal{T};x,t)\left\{\theta\left[v_D\left(t+\frac{\mathcal{T}}{2}\right)-x-\frac{\mathcal{X}}{2}\right]-\theta(x_- - x-\frac{\mathcal{X}}{2})\right\}. \tag{A2}
$$

According to the Fourier convolution formula,

$$
\mathscr{F}[f_1(\mathcal{T})\cdot f_2(\mathcal{T})] = \frac{1}{2\pi}\mathcal{F}_1(\omega) * \mathcal{F}_2(\omega) = \int \mathcal{F}_1(\omega')\mathcal{F}_2(\omega-\omega')\,d\omega', \tag{A3}
$$

where $\mathscr{F}[f(t)] = \int e^{i\omega t} f(t)\, dt = \mathcal{F}(\omega)$. Equation (A2) can be rewritten as

$$I = \frac{J_{ex}}{4\pi} \int dk' \int \hat{\Theta}_1(k', \omega'; x, t) \hat{G}^<(k - k', \omega - \omega'; x, t)\, d\omega', \tag{A4}$$

with

$$\hat{\Theta}_1(k, \omega; x, t) = \int d\mathcal{X} e^{-ik\mathcal{X}} \int d\mathcal{T} e^{i\omega\mathcal{T}} \boldsymbol{M}_1 \cdot \hat{\boldsymbol{\sigma}} \left\{ \theta\left[v_D\left(t + \frac{\mathcal{T}}{2}\right) - x - \frac{\mathcal{X}}{2} \right] - \theta\left(x_- - x - \frac{\mathcal{X}}{2} \right) \right\}, \tag{A5}$$

which can be interpreted as the transition probability of the momentum and frequency from (k, ω) jumping to $(k - k', \omega - \omega')$. It is not hard to get the expression for $\hat{\Theta}_1(k', \omega'; x, t)$:

$$\hat{\Theta}_1(k', \omega'; x, t) = -\frac{2\pi}{ik'} \boldsymbol{M}_1 \cdot \hat{\boldsymbol{\sigma}} [e^{-2ik'(v_D t - x)} \delta(k' v_D - \omega') - e^{-2ik'(x_- - x)} \delta(\omega')]. \tag{A6}$$

Then the equation satisfied by the lesser Green's function beyond the gradient approximation can be obtained:

$$\begin{aligned}
&i\hbar \left[\frac{\partial}{\partial t} + \frac{\hbar k}{m_e} \nabla_x - \frac{eE}{\hbar} \nabla_k \right] \hat{G}^<(k, \omega; x, t) + \frac{J_{ex}}{4\pi} \int dk' \int d\omega'\, \hat{\Theta}_1(k', \omega'; x, t) \hat{G}^<(k - k', \omega - \omega'; x, t) \\
&\quad - \frac{J_{ex}}{4\pi} \int dk' \int d\omega'\, \hat{G}^<(k - k', \omega - \omega'; x, t) \hat{\Theta}_2(k', \omega'; x, t) \\
&\quad + \frac{J_{ex}}{4\pi} \int dk' \int d\omega'\, \hat{\Theta}_3(k', \omega'; x, t) \hat{G}^<(k - k', \omega - \omega'; x, t) \\
&\quad - \frac{J_{ex}}{4\pi} \int dk' \int d\omega'\, \hat{G}^<(k - k', \omega - \omega'; x, t) \hat{\Theta}_4(k', \omega'; x, t) \\
&= \int d\mathcal{X}\, e^{-ik\mathcal{X}} \int d\mathcal{T}\, e^{i\omega\mathcal{T}} \int dx_3\, [\Sigma_t G^< - \Sigma^< G_{\bar{t}} - G_t \Sigma^< + G^< \Sigma_{\bar{t}}] \\
&= -\left(\frac{\partial f}{\partial t} \right)_{\text{collision}}.
\end{aligned} \tag{A7}$$

$\hat{\Theta}_2$, $\hat{\Theta}_3$, and $\hat{\Theta}_4$ can be obtained in the same way as Eq. (A2) and have the following forms:

$$\hat{\Theta}_2(k', \omega'; x, t) = \frac{2\pi}{ik'} \boldsymbol{M}_1 \cdot \hat{\boldsymbol{\sigma}} [e^{-2ik'(x - v_D t)} \delta(k' v_D - \omega') - e^{-2ik'(x - x_-)} \delta(\omega')], \tag{A8}$$

$$\hat{\Theta}_3(k', \omega'; x, t) = \frac{2\pi}{ik'} \boldsymbol{M}_2 \cdot \hat{\boldsymbol{\sigma}} [e^{-2ik'(v_D t - x)} \delta(k' v_D - \omega') - e^{-2ik'(x_+ - x)} \delta(\omega')], \tag{A9}$$

$$\hat{\Theta}_4(k', \omega'; x, t) = -\frac{2\pi}{ik'} \boldsymbol{M}_2 \cdot \hat{\boldsymbol{\sigma}} [e^{-2ik'(x - v_D t)} \delta(k' v_D - \omega') - e^{-2ik'(x - x_+)} \delta(\omega')]. \tag{A10}$$

In addition, the collision terms on the right side of Eq. (A7), including the momentum relaxation of electrons and spin-flip relaxation, are simplified by the relaxation time approximation [24] instead of the Kadanoff-Baym gradient expansion used by Mahan [28]:

$$\left(\frac{\partial \hat{f}}{\partial t} \right)_{\text{collision}} = \left(-\frac{\partial f^0}{\partial \epsilon} \right) \left[\frac{f\hat{I} + \boldsymbol{g} \cdot \hat{\boldsymbol{\sigma}} - \langle f\hat{I} + \boldsymbol{g} \cdot \hat{\boldsymbol{\sigma}} \rangle}{\tau} + \frac{2\langle \boldsymbol{g} \cdot \hat{\boldsymbol{\sigma}} \rangle}{\tau_{sf}} \right], \tag{A11}$$

where τ is the momentum relaxation time and τ_{sf} is the spin-flip relaxation time.

By using the relation in Eq. (2), $\hat{G}^<$ in Eq. (A7) can be replaced by the Wigner distribution function $\hat{f}(k, \omega; x, t)$; further, by inserting Eq. (A6) and Eqs. (A8)–(A10) into Eq. (A7), we can obtain the equation satisfied by the Wigner distribution function:

$$\begin{aligned}
&\left(\frac{\partial}{\partial t} + \frac{\hbar k}{m_e} \nabla_x - \frac{eE}{\hbar} \nabla_k \right) \hat{f}(k, \omega; x, t) + \frac{J_{ex}}{2\hbar} \int \frac{1}{k'} (\boldsymbol{M}_1 - \boldsymbol{M}_2) \cdot \hat{\boldsymbol{\sigma}} \hat{f}(k - k', \omega - k' v_D; x, t) e^{-2ik'(v_D t - x)}\, dk' \\
&\quad + \frac{J_{ex}}{2\hbar} \int \frac{1}{k'} \hat{f}(k - k', \omega - k' v_D; x, t) (\boldsymbol{M}_1 - \boldsymbol{M}_2) \cdot \hat{\boldsymbol{\sigma}} e^{-2ik'(x - v_D t)}\, dk' \\
&\quad - \frac{J_{ex}}{2\hbar} \int \frac{1}{k'} (\boldsymbol{M}_1 e^{-2ik'(x_- - x)} - \boldsymbol{M}_2 e^{-2ik'(x_+ - x)}) \cdot \hat{\boldsymbol{\sigma}} \hat{f}(k - k', \omega; x, t)\, dk' \\
&\quad - \frac{J_{ex}}{2\hbar} \int \frac{1}{k'} \hat{f}(k - k', \omega; x, t) (\boldsymbol{M}_1 e^{-2ik'(x - x_-)} - \boldsymbol{M}_2 e^{-2ik'(x - x_+)}) \cdot \hat{\boldsymbol{\sigma}}\, dk' \\
&= \left(\frac{\partial \hat{f}}{\partial t} \right)_{\text{collision}}.
\end{aligned} \tag{A12}$$

By inserting Eqs. (3) and (A11) into the above formula and using a series of procedures that is rigorous but cumbersome we can get the coupled SBEs (4) and (5) for the scalar distribution function $f(k, \omega; x, t)$ and vector distribution function $\boldsymbol{g}(k, \omega; x, t)$.

[1] R. Sbiaa and S. N. Piramanayagam, Appl. Phys. A **114**, 1347 (2014).
[2] P. Lendecke, R. Eiselt, G. Meier, and U. Merkt, J. Appl. Phys. **103**, 073909 (2008).
[3] J. Yoon, J. C. Lee, C. Y. You, S. B. Choe, K. H. Shin, and M. H. Jung, IEEE Trans. Magn. **44**, 2527 (2008).
[4] X. S. Wang, P. Yan, Y. H. Shen, G. E. W. Bauer, and X. R. Wang, Phys. Rev. Lett. **109**, 167209 (2012).
[5] J. C. Slonczewski, J. Magn. Magn. Mater. **159**, L1 (1996).
[6] L. Berger, Phys. Rev. B **54**, 9353 (1996).
[7] O. Boulle, G. Malinowski, and M. Klaui, Mater. Sci. Eng., R **72**, 159 (2011).
[8] J. Grollier, P. Boulenc, V. Cros, A. Hamzic, A. Vaures, A. Fert, and G. Faini, Appl. Phys. Lett. **83**, 509 (2003).
[9] M. Yamanouchi, D. Chiba, F. Matsukura, and H. Ohno, Nature (London) **428**, 539 (2004).
[10] D. Jiles, *Introduction to Magnetism and Magnetic Materials*, 3rd ed. (CRC Press, Boca Raton, 2015), pp. 1–46.
[11] J. Sampaio, J. Grollier, and P. J. Metaxas, *Magnetism of Surfaces, Interfaces, and Nanoscale Materials*, Handbook of Surface Science Vol. 5 (North-Holland, Amsterdam, 2015), pp. 335–370.
[12] L. Berger, J. Appl. Phys. **55**, 1954 (1984).
[13] L. Berger, J. Appl. Phys. **49**, 2156 (1978).
[14] Z. Li and S. Zhang, Phys. Rev. Lett. **92**, 207203 (2004).
[15] J. Zhang and P. M. Levy, Phys. Rev. B **71**, 184426 (2005).
[16] A. Shpiro, P. Levy, and S. Zhang, Phys. Rev. B **67**, 104430 (2003).
[17] R. E. Camley and J. Barnaś, Phys. Rev. Lett. **63**, 664 (1989).
[18] J. Barna, A. Fuss, R. E. Camley, P. Grunberg, and M. Zinn, Phys. Rev. B **42**, 8110 (1990).
[19] T. Valet and A. Fert, Phys. Rev. B **48**, 7099 (1993).
[20] S. Zhang and P. M. Levy, Phys. Rev. B **57**, 5336 (1998).
[21] L. Kadanoff, G. Baym, and S. Rice, Phys. Today **16**(3), 60 (1963).
[22] L. Sheng, D. Y. Xing, Z. D. Wang, and J. Dong, Phys. Rev. B **55**, 5908 (1997).
[23] L. Sheng, H. Y. Teng, and D. Y. Xing, Phys. Rev. B **58**, 6428 (1998).
[24] J. Zhang, P. M. Levy, S. Zhang, and V. Antropov, Phys. Rev. Lett. **93**, 256602 (2004).
[25] Z. Wang, Eur. Phys. J. B **86**, 206 (2013).
[26] Z. Wang, Phys. A (Amsterdam, Neth.) **465**, 754 (2017).
[27] E. Wigner, Phys. Rev. **40**, 749 (1932).
[28] G. D. Mahan, Phys. Rep. **145**, 251 (1987).
[29] J. Rammer and H. Smith, Rev. Mod. Phys. **58**, 323 (1986).
[30] M. Elidrissi, S. Bastrukov, H. Wang, J. Khoo, K. S. Chan, and K. Eason, IEEE Trans. Magn. **49**, 2610 (2013).
[31] C. Yang, Z.-C. Wang, Q.-R. Zheng, and G. Su, Eur. Phys. J. B **92**, 136 (2019).
[32] R. Bellman, *Stability Theory in Differential Equations* (Dover, New York, 1969), pp. 75–92.
[33] D. H. Sattinger, *Topics in Stability and Bifurcation Theory* (Springer, Berlin, 1973), pp. 125–140.